HHS Public Access

Author manuscript

Proteins. Author manuscript; available in PMC 2020 May 01.

Published in final edited form as:

Proteins. 2019 May ; 87(5): 401–415. doi:10.1002/prot.25662.

Chaperone-like activity of the N-terminal region of a human small heat shock protein and chaperone-functionalized nanoparticles

Emily F. Gliniewicz[†], **Kelly M. Chambers**, **Elizabeth R. De Leon**[†], **Diana Sibai**[†], **Helen C. Campbell**[†], and **Kathryn A. McMenimen**

Department of Chemistry, Mount Holyoke College, South Hadley, Massachusetts

Abstract

Small heat shock proteins (sHsps) are molecular chaperones employed to interact with a diverse range of substrates as the first line of defense against cellular protein aggregation. The N-terminal region (NTR) is implicated in defining features of sHsps; notably in their ability to form dynamic and polydisperse oligomers, and chaperone activity. The physiological relevance of oligomerization and chemical-scale mode(s) of chaperone function remain undefined. We present novel chemical tools to investigate chaperone activity and substrate specificity of human HspB1 (B1NTR), through isolation of B1NTR and development of peptide-conjugated gold nanoparticles (AuNPs). We demonstrate that B1NTR exhibits chaperone capacity for some substrates, determined by anti-aggregation assays and size-exclusion chromatography. The importance of protein dynamics and multivalency on chaperone capacity was investigated using B1NTR-conjugated AuNPs, which exhibit concentration-dependent chaperone activity for some substrates. Our results implicate sHsp NTRs in chaperone activity, and demonstrate the therapeutic potential of sHsp-AuNPs in rescuing aberrant protein aggregation.

Keywords

molecular chaperone; mutagenesis; nanotechnology; protein chemistry; small heat shock protein (sHsp)

1 | INTRODUCTION

Small heat shock proteins (sHsps) are molecular chaperones, generally considered to be among the first line of defense against cellular stress.[1,2] These ubiquitous and abundant sHsps interact with partially folded substrate (also known as target or client) proteins to

Correspondence, Kathryn A. McMenimem, Department of Chemistry, Mount Holyoke College, 50 College Street, South Hadley, MA 01075, USA, kamcmeni@mtholyoke.edu.

[†]Undergraduate co-author.

CONFLICT OF INTEREST

The authors declare that they have no conflicts of interest with the contents of this article.

The content is solely the responsibility of the authors and does not necessarily represent the official views of the National Institutes of Health.

SUPPORTING INFORMATION

Additional supporting information may be found online in the Supporting Information section at the end of the article.

stabilize and prevent their aggregation.[3] sHsps are relatively promiscuous when selecting their substrates, functioning under constitutive conditions as well as in response to various stress signals.[4,5] The sHsp family has diverse cellular functions, including their involvement in the proteostasis network as well as playing distinct roles in cellular pathways. HspB1 (Hsp27) is an important member of the sHsp family and has been implicated in diverse cellular processes, particularly in human tissues. Its ability to interact with non-native protein states suggests a major role in preventing aberrant substrate aggregation.[6,7]

Several structural features of sHsps are thought to contribute to their chaperone function. Each sHsp is comprised of N- and C-terminal regions (NTR, CTR) which flank the highly conserved α-crystallin domain (ACD) of approximately 90 Amino acids, a defining characteristic of all sHsps (Figure 1A, B).[1,8,9] Dimer formation occurs at an interface formed by the ACD. Removal of the NTR and CTR has resulted in crystal and NMR structures for several mammalian ACDs.[10] A conserved ACD topology of a 6- or 7-stranded β-sandwich forms a dimer interface with anti-parallel β-strands, which acts as a basic building block for oligomer formation. Unlike the ACD, the NTR and CTR vary both in length and sequence among the sHsps. The NTR and CTR are implicated in regulating inter-subunit interactions and higher-order oligomerization, and have also been shown to facilitate interactions with diverse substrate proteins.[11–13] A defining feature of sHsps is in their ability to assemble into polydisperse oligomers of varying shape and size, which exhibit subunit exchange at physiological temperatures and result in dynamic protein ensembles.[3,14] The formation of these ensembles likely contributes to chaperone activity, although the exact mechanisms remain unknown. The current hypothesis suggests that sHsps bind partially denatured substrates via exposed hydrophobic surfaces in order to “kinetically partition” the substrate from interacting with other metastable species, binding instead to sHsp hydrophobic surfaces. Some mechanistic models propose the stress-induced “release” of sHsp dimers from the oligomeric species, which can then interact with partially denatured or non-native substrates.[15] These small complexes are able to reassemble with sHsp oligomers to form larger sHsp–client protein complexes.

Many studies have attempted to identify the molecular and sequence-specific regions of sHsps that underlie chaperone function, with the majority suggesting a pivotal role for the N-terminal region (NTR). Studies focusing on the canonical sHsps, human HspB1, HspB4, and HspB5, have identified several sequences within the NTR that contribute to chaperone activity. Contradictory reports suggest that there may be more than one sequence within the NTR that contributes to chaperone activity.[13,16–18] It is probable that mutagenesis experiments would be complicated by the overlapping role of the sHsp NTR in higher-order oligomeric dynamics. These dual roles are challenging to deconvolute when assessing the impact of sequence specificity on NTR function. In addition to these challenges, evaluating the role of higher-order oligomers, multivalency, and available 3D surface properties of sHsps will contribute to our understanding of the mechanism of action of sHsps, which currently remains unknown. HspB1 exhibits concentration-dependent oligomerization, where chaperone activity increases as concentration decreases, suggesting that the dimer is more active than larger oligomers. The NTR is proposed to be more exposed in this state.[19–24] Mutagenesis studies with physiologically relevant phosphorylation mimics (S → D mutations) at three different positions in the NTR have resulted in an increase in dimers and

small oligomers, with a corresponding increase in chaperone activity.[25–27] Recently, a soluble, truncated, ACD-only structure of HspB1 was solved, highlighting the role of a redox-sensing cysteine residue in altering protein structure and, in turn, modulating chaperone activity.[10] Importantly, sHsp chaperone activity is retained in ACD-only and truncated structures, suggesting redundancy may be important for chaperone activity.[22,23,28]

Several in vitro studies have sought to identify sequences or regions that define sHsp chaperone activity, which is characterized by its interactions with substrates that prevent or decrease aggregation.[29–31] Many studies support the central role of the NTR in substrate-binding, providing further evidence that multiple substrate-interacting domains are present, though there are conflicting results about which sequences are active.[29–31] While these differences are sometimes attributed to poor sequence conservation across species, there is a highly conserved region of the NTR among vertebrate sHsps. Others propose that the dual role of the NTR in oligomeric assembly and chaperone activity is likely to contribute to differences in these reports.[12] Structural conformations of the NTR (88 amino acids, Figure 1B) are more varied than those observed for the ACD. The NTR is influenced by oligomeric assembly and dynamics of the full-length sHsp, exhibiting both extended and compact structures under different conditions.[14,32] For example, HspB6, which naturally dimerizes, is proposed to have a compact and exposed NTR in solution.[33] Recently, efforts to map interaction sites on the substrate, malate dehydrogenase (MDH), and another sHsp, yeast Hsp26, have identified several sites throughout each protein. Sites within the NTR, ACD, and CTR of Hsp26 were identified, and interacting regions were distributed across the denatured MDH surface.[34] Additional studies have used both chemical and photo-crosslinking methods to identify sHsp-substrate interacting regions across a variety of sHsps from different organisms. They have concluded that the NTR is the primary site of substrate binding, although binding to the ACD and CTR occurs and may mediate interactions under different stress conditions.[35–37] Furthermore, it is possible that sHsps utilize a hierarchical mechanism to activate multiple substrate interacting sites under various stress conditions in order to maintain the integrity of cellular proteostasis.[38,39]

Importantly, recent models highlight the diverse physiological roles of sHsps necessary to maintain the proteostasis network, expanding beyond substrate binding alone. Specifically, sHsps have likely broadened their roles beyond “holdase” activity and the prevention of large aggregate formation. Recent studies using yeast sHsps demonstrate that two sHsps (Hsp26 and Hsp42) utilize distinct mechanisms to establish a comprehensive system for combating protein misfolding. Interestingly, one of the yeast sHsps (Hsp42) is actively involved in aggregase activity. Hsp42 induces co-aggregation with a denaturing substrate early on, ultimately leading to more soluble and less toxic aggregates. This activity is dependent on interactions with Hsp26 NTR.[34,40] Due to the dynamic nature of sHsp oligomeric architecture, the dual role of the NTR, and the variety of client proteins that sHsps interact with under physiological conditions, it is likely that several sequences within each sHsp contain chaperone activity.[14,42] Additionally, it is plausible that chaperone activity may manifest as a combination of interactions with a single substrate.[12,41]

Chaperone activity (defined as anti-aggregation activity for sHsps) is measured experimentally, in vitro, using model substrates under conditions that induce protein

unfolding and aggregation.[42] Previous studies have identified functional "mini-chaperones," which correspond to a small fragment (~20 residues) from the ACD of several mammalian sHsps. These mini-chaperones exhibit in vitro chaperone activity in addition to other protective properties.[43–47] Substrate binding sites in the ACD of mini-chaperones are markedly hydrophobic.[28,43,48] In addition to sites in the ACD, the flanking NTR is implicated in substrate binding, likely contributing to the versatility of sHsp substrate binding through hydrophobic and other interactions.[11,49] Reflecting upon these observations from previous studies, we hypothesized that the NTR, in the absence of both the ACD and CTR, may possess chaperone activity. The protective effects of the ACD-derived mini-chaperones suggest their potential to function as therapeutics for human diseases associated with protein aggregation. Further identification of additional peptides exhibiting chaperone activity may advance the development of such therapeutics.

Here, we establish that the human HspB1 N-terminal region (B1NTR) alone (ie, the NTR in the absence of the ACD or CTR) can interact with substrates in vitro to exhibit chaperone activity. We thus identify, for the first time, a truncated region outside of the ACD with this ability. Further, we examine the chaperone activity of B1NTR toward different substrates. B1NTR exhibits varying activity toward each substrate protein, measured as the degree to which aggregation of the substrate is suppressed. Overall, we observe that B1NTR is a more effective chaperone for MDH and Lys, compared to CS. These results suggest that the NTR of this sHsp contributes to substrate selectivity by interacting with substrates at different times during the aggregation process. Finally, we investigate the role of multivalency in sHsp-substrate interactions by conjugating B1NTRs to 10 nm and 5 nm gold nanoparticles (AuNPs) resulting in stable, multivalent, peptide-conjugated AuNPs ("artificial sHsps") that replicate in vitro chaperone activity and substrate selectivity.[50–54] These B1NTR–AuNPs also exhibit varying substrate selectivity, influenced both by B1NTR and the relative size of the AuNP. Our NTR–AuNPs are promising candidates for exploring the molecular mechanisms of ATP-independent chaperone activity. These artificial sHsps provide tools to investigate the molecular mechanisms of sHsp–client interactions decoupled from sHsp oligomer dynamics, while also investigating the importance of the NTR in contributing to general chaperone activity.

2 | MATERIALS/EXPERIMENTAL DETAILS

2.1 | Peptides, proteins, and reagents

MDH was obtained from EMD Millipore. Lysozyme (Lys) and citrate synthase (CS) were procured from Sigma-Aldrich. HALT protease inhibitor cocktail was purchased from Fisher Scientific. Unconjugated citrate-coated AuNPs, PEGylated gold nanoparticles (PEG-NP), and high and low density purified sHsp-conjugated AuNPs (B1NTR-NP) were obtained from Nano Hybrids (Austin, TX). Prior to HspB1NTR conjugation, a PEG linker was attached to the AuNP to increase NP stability. The resulting NPs were stored in 1× PBS with 0.05% Tween and characterized by DLS and TEM (Supporting Information).

2.2 | Protein expression and purification

The NTR (residues 1–88) of HspB1 with an inserted N-terminal cysteine (B1NTR) was expressed from the pMCSG7 vector after ligation independent cloning (gifted by Dr. Jason Gestwicki, UCSF). HspB1NTR was designed with an N-terminal cysteine residue for use in several downstream applications. The first was to facilitate the coupling of the peptide to the surface of AuNPs using thiol–gold interactions.[55] In future studies, incorporating a label for B1NTR may be necessary, and the presence of a single cysteine would create a site-specific chemical "handle" for labeling experiments. Furthermore, wild-type HspB1 does contain a single cysteine within the ACD, indicating the presence of a cysteine residue is not out of place in the context of potential HspB1-substrate interactions. All recombinant sHsps were expressed in *Escherichia coli* BL21 (DE3), cultured in LB media containing 100 μg/mL ampicillin or 50 μg/mL kanamycin (wild-type HspB1), as previously described.[56] Protein expression was induced with the addition of isopropyl thio-β-D-thiogalactoside to a final concentration of 0.5 mM at 25°C for 5 h. Wild-type HspB1 was purified by methods previously described.[57] Recombinant human HspB1 was expressed in *E. coli* BL21 (DE3) cells using plasmids kindly gifted by Dr. Jason Gestwicki (UCSF). Cells were first spun down at 11 000 RCF at 4°C for 15 min, and then resuspended in lysis buffer (20 mM Tris, 100 mM NaCl, 6 M urea, 5 mM β-mercaptoethanol, 15 mM imidazole, pH 8.0) with the addition of a cocktail protease inhibitor. Resuspended cells were sonicated for 6 intervals of 30 s with 30 s breaks in between. The lysed cells were then spun again at 20 000 RCF and 4°C for 45 min. All proteins were purified from lysate using Ni^{2+} affinity columns. Resulting proteins were exchanged into 25 mM sodium phosphate and 100 mM sodium chloride buffer (pH 7.4), and then underwent further purification by SEC in 1x PBS (pH 7.4). Protein concentration was determined using the Thermo Scientific BCA assay kit and NanoDrop One UV/Vis Spectrometer (Thermo Scientific).

2.3 | CD-spectroscopy

B1NTR was diluted to 0.24 mg/mL in PBS. CD spectra were recorded in a Jasco J-1500 Spectrometer (Jasco Co., Tokyo, Japan) at 24°C. Far UV CD spectra were recorded using a cuvette with 1 mm path length at 0.5 nm intervals between 190 and 250 nm. The spectra were taken as the average of 15 scans recorded at a speed of 100 nm/min.

2.4 | Chaperone-like activity assay

To determine whether the NTR of HspB1 modulates chaperone function, B1NTR, B1NTR-NPs, and corresponding controls (HspB1, PEGNPs, citrate-NPs) were independently mixed with two heat-denatured substrate proteins, MDH and CS. CS aggregation assays were performed using 2.5 μM of substrate in 0.1 mL PBS (pH 7.4) at 45°C, in both the absence and presence of B1NTR, B1NTR-NP, wild-type HspB1, or other indicated controls. MDH aggregation assays were performed using 15 μM of substrate in 0.1 mL PBS (pH 7.4) at 45°C, in the absence and presence of B1NTR, B1NTR-NP, wild-type HspB1, or other indicated controls. The DTT-induced aggregation of Lys was also observed in 1× PBS (pH 7.4). Lys (35 μM) was denatured in the presence of 20 mM DTT in a clear bottom 96-well plate. Aggregation was monitored at 340 nm in a Molecular Devices M5e multi-mode plate reader under constant temperature (37°C), while shaking for 10 s between each read. All

assays were normalized based on the maximum absorbance of the averaged substrate (CS, MDH, and Lys) curves.

2.5 | Chaperone and substrate solubility gel

Samples obtained from the chaperone-like activity assay (0.5 mL) were centrifuged at 13 000 RPM for 3 min, repeated twice. The soluble and pelleted fractions were collected separately. Following this, 1× non-reducing sample loading buffer was added to each sample. MDH samples and controls were run on 10% mini-PROTEAN TGX precast gels (Bio-Rad). CS samples and controls were run on 8–16% gradient mini-PROTEAN TGX precast gels (Bio-Rad). Lys samples and controls were run on a 10% mini-PROTEAN TGX precast, stain-free gel. All gels were run for 40 min at 160 V. The gels were silver stained according to the protocol specified in the Pierce Silver Stain kit (Thermo scientific).

2.6 | Size-exclusion chromatography

Changes in protein complex size arising from the interaction of B1NTR with substrate proteins were analyzed by size-exclusion chromatography (SEC). Samples were prepared using equimolar ratios of B1NTR and substrate, as indicated. Concentrations varied for each substrate, 5 μM CS, 50 μM MDH, or 75 μM Lys, and were mixed with indicated amounts of B1NTR. Each sample (1 mL) was heated at 45°C for 1 h, then cooled to room temperature. Following this, 200 μL of each sample was loaded on to a Superdex 200 10/300 increase or Superose 6 10/300 increase column, equilibrated with PBS (pH 7.4) and attached to an AKTA Pure 25 (GE Healthcare, Pittsburgh, PA). The column was run at 4°C with a flow rate of 0.3 mL/min. Previously, each column had been calibrated with the following protein markers: thyroglobulin (669 kDa), γ-globulin (158 kDa), ovalbumin (44 kDa), myoglobin (17 kDa), and vitamin B12 (1.35 kDa), to generate a standard curve (see Supporting Information Figure S2).

2.7 | 1,8-ANS (ANS) binding studies

A stock solution (20 mM) of 1,8-ANS (1-anilinonaphthalene-8-sulfonic acid, Sigma-Aldrich) was dissolved in DMSO and diluted using 1× PBS to a 100 μM final concentration for each assay. The binding assay was performed by combining B1NTR (15 mM final concentration) with ANS for 1 h at either 25°C, 45°C, or 55°C. Fluorescence was measured in a 96-well, black, flat-bottom, polypropylene plate (Fisherbrand) on a M5e multi-mode plate reader (Molecular Devices). The solutions were excited at 375 nm and emission intensities were measured from 400 to 600 nm. All values are measured in arbitrary units and were normalized to the highest value for ANS binding to B1NTR at 25°C. Each curve is the average of ≥3 independent trials.

3 | RESULTS

3.1 | B1NTR characterization

Previous studies have implicated sHsp NTRs in chaperone activity and suggest that varying lengths and physiochemical properties contribute to substrate selectivity.[12,24,58] Therefore, we investigated the chaperone-like activity of B1NTR to determine if this region of a human sHsp affected anti-aggregation activity in vitro, independently of the ACD and CTR.

Production of the full-length NTR (residues 1–88) of human HspB1 was performed using standard recombinant protein expression and purification, resulting in a peptide fragment of ~9.5 kDa (Figure 1C).

sHsp NTRs are generally considered to have relatively few secondary or other structural elements, especially compared to the ACD. There are several different reports on the location and exposure of the NTR in the context of small and large oligomeric assemblies. This suggests that many three-dimensional conformations are likely to be attributed to this region of the protein and are influenced by various factors such as concentration, substrates, and post-translational modifications.[15,23] We performed CD spectroscopy of soluble B1NTR(0.24 mg/mL) to identify the presence of secondary structural elements. CD data were processed using two methods. The first, described by Raussens et al.,[59] resulted in secondary structure identification of: 6.5% β-strand, 25.9% turn, 12.5% random, and 39.1% other structural elements. The second method, CAPITO, described by Weidemann et al.,[60] reported secondary structural elements: 26% helix, 13% β-strand, and 61% irregular. For comparison, based on the sequence of B1NTR, CAPITO predicted the structure of B1NTR would be 24% helix, 0% β-strand, and 76% irregular, according to the Chou–Fasman algorithm (Supporting Information Figure S1).[60] Overall, our CD data primarily indicate the presence of irregular or unstructured elements in addition to small percentage of α-helical elements, which was previously undetermined.

Full-length sHsps exhibit concentration-dependent structural changes. To determine if similar structural alterations are observed in the absence of the ACD and CTR, we monitored concentration-dependent changes in B1NTR structure using SEC and SDS-PAGE (Figure 2A,B). All samples were prepared using the same protein stock solution and were diluted to the final concentrations indicated (Figure 2A). At low concentrations of B1NTR (25 μM, 0.24 mg/mL), a small peak (Peak A) was observed by SEC in addition to a monomer form, which was observed at ~9.5 kDa by SDS-PAGE (Peaks B,C). In the gel, Peak A did not indicate the presence of any protein, suggesting negligible protein was eluted. (Figure 2B). The peaks and corresponding gel fractions observed for 25 μM B1NTR indicate less relative protein compared to the samples prepared at higher concentrations (50 and 150 μM, 0.48 and 1.45 mg/mL, respectively), which would be expected. The elution peaks do not shift as a result of concentration changes, indicating the protein is not forming significant oligomers in response to changes in concentration, unlike full length sHsps. There is a small peak eluting at ~21.5 mL (Figure 2A,B, Peak D), which likely corresponds to a minor contaminant (lane D). At all concentrations, a band was observed by SDS-PAGE (~10 kDa), corresponding to B1NTR (Figure 2B lanes B,C). Overall, fraction samples shown in Figure 2B identify B1NTR eluting over a ~2 mL broad peak, which likely arises from varying protein conformations. A standard curve was obtained for calibration of the gel filtration columns prior to evaluating B1NTR samples (see Supporting Information Figure S2).

The hydrophobic core of B1NTR was analyzed using fluorescence changes in 8-anilinonaphthalene-1-sulfonic acid (ANS) binding before and after heating (see Supporting Information Figure S3). A decrease in ANS fluorescence is observed as temperature increases from 25 to 45°C, which suggests B1NTR contains exposed hydrophobic regions in

solution. We hypothesize that B1NTR is reorganized to minimize unfavorable hydrophobic interactions at low temperature, which is consistent with the CD data suggesting unstructured elements are present. At higher temperature, some reorganization occurs to expose these hydrophobic surfaces and decrease ANS intensity. This would be consistent with prior data indicating other truncated sHsps form unstable structures in solution.[12,13]

3.2 | Chaperone activity of soluble B1NTR

The in vitro chaperone activity of B1NTR compared to full-length wild-type HspB1 was investigated using three model substrates, MDH, CS, and Lys. Heat-induced aggregation of MDH and CS, and DTT-induced aggregation of Lys was used to measure the chaperone activity of B1NTR and HspB1. These substrates are widely used to characterize sHsp chaperone activity and enable broad comparisons in client protein–sHsp interactions due to differences in denaturing requirements of each substrate. Given that sHsps are oligomeric ensembles, several ratios of substrate to chaperone were compared to identify potential trends in the relative amount of chaperone protein required to provide significant anti-aggregation activity in solution. A panel of controls demonstrates the stability of B1NTR and wild-type HspB1 upon heating to 55°C (see Supporting Information, Figure S4).

When CS was investigated as the denatured client protein, B1NTR exhibited a dose-dependent suppression of aggregation (Figure 3A), as revealed by light scattering measurements. An equimolar ratio of CS to B1NTR led to an initial increase in aggregation, whereas increasing the amount of chaperone to a 1:6 (CS: B1NTR) ratio resulted in a >80% suppression of light scattering. Compared to full-length HspB1, B1NTR is less active when preventing the aggregation of CS (Figure 3A). This is not surprising, as there is likely more than one interacting site on the full-length sHsp.[34] Additionally, different oligomerization states observed for wild-type HspB1 may play a role in substrate binding. Both of these features of full-length HspB1 are absent in B1NTR. The chaperone activity of B1NTR at low concentrations, specifically with 1:1 and 1:3 ratios of CS to B1NTR, altered the lag phase and overall aggregation of CS (Figure 3A). The 6-fold increase in aggregation suggests that B1NTR is interacting with CS during the unfolding phase at low concentrations and co-aggregating with the substrate. This observation is also supported by SDS-PAGE analysis. In the case of CS, this contributes to an overall decrease in the protective capacity of B1NTR at low concentrations of chaperone, relative to substrate. Wild-type HspB1 also permits an increase in initial aggregation of CS, however, the overall protective capacity is higher compared to B1NTR. Interestingly, this would be consistent with the requirement of additional substrate-interacting sites in the ACD or CTR of HspB1 in order to maintain the protective capacity of HspB1 for CS.

The heat-induced aggregation of MDH was suppressed in a dose-dependent manner by B1NTR (Figure 3B), which demonstrated significant chaperone activity. Intriguingly, B1NTR is a more active chaperone for MDH when compared to full-length HspB1 at a 1:1 (substrate:chaperone) ratio. The kinetics of chaperone function are different for B1NTR than for HspB1, revealed by an initial increase in the aggregation rate of MDH, which slows significantly after ~5 min in time-dependent aggregation experiments. This change in the lag-phase of aggregation indicates that B1NTR may interact with MDH during unfolding to

change the pathway relative to that exhibited in the absence of a chaperone. Wild-type HspB1 also increases initial aggregation of MDH, similar to B1NTR. However, the total protective capacity of B1NTR is greater than wild-type HspB1 at similar concentration ratios. While this result is surprising, there are reports of other NTR mutations leading to an increase in chaperone protective capacity compared to wild-type sHsps.[12] The increase in protective capacity of B1NTR may arise from the combined effects of changing the initial unfolding pathway of MDH and from the allowance of more efficient substrate interactions, compared to wild-type HspB1. We hypothesize that role of the NTR in oligomeric assembly, when attached to the ACD and CTR, may contribute to the regulation of sHsp–substrate binding, and for some substrates, decrease the substrate–chaperone interactions. This would provide a possible mechanism to account for the increase in chaperone capacity of B1NTR. In the absence of the ACD and CTR, there is no regulatory mechanism to prevent earlier association between the NTR and substrate. The regulatory effect of sHsp oligomerization may be physiologically important during cellular stress, so as to impart control on both the number and type of substrate–chaperone interactions. Importantly, B1NTR exhibits increased protective capacity for MDH compared to CS (Figure 3A,B), indicating possible substrate selectivity for denaturing MDH relative to CS. This would indicate that the regulatory effects of sHsp oligomerization are not equally important for all substrates in vitro. Differences in the protective capacity of NTR mutations have been previously described for other sHsps and indicate that chaperone activity is not equivalent for all substrates, potentially contributing to divergent physiological roles for each sHsp.[12]

Evaluating the DTT-induced denaturation of Lys was particularly important for characterizing the substrate selectivity and chaperone activity of B1NTR. This allowed for a comparison of substrates that denature under varying mechanisms in order to begin probing the effect of a range of conditions on sHsp chaperone activity. Overall, B1NTR exhibits chaperone activity for Lys, where a 1:1 ratio of Lys: B1NTR decreases substrate aggregation by ~50%. The protective capacity of B1NTR is similar for both MDH and Lys. However, unlike the chaperone activity displayed with CS or MDH, the lag phase of Lys aggregation was unaffected by B1NTR. We observed changes in the onset of aggregation (lag phase) when CS and MDH were the substrates and no variation when Lys was a substrate, This indicates that the protective capacity of B1NTR had little to no effect on Lys unfolding, and that the chaperone capacity of B1NTR manifested only in preventing subsequent aggregation. Unlike CS and MDH, which undergo heat-denatured unfolding, Lys aggregation is induced by the reduction of disulfide bonds by DTT. This difference in the nature of substrate unfolding may contribute to the mechanism(s) of chaperone capacity of the sHsp NTR, which would be consistent with the model describing a hierarchical mechanism of sHsp–substrate binding and chaperone activity. Surprisingly, B1NTR is a more active chaperone than wild-type HspB1 under similar conditions (Figure 3C). These results suggest that the oligomeric organization of HspB1 potentially affect chaperone activity and that the oligomeric dynamics may affect sHsp activity in a substrate-specific manner, resulting in reduced activity. A model where available sHsp substrate binding sites are regulated or modulated by sHsp oligomer dynamics could account for the increase in activity of B1NTR relative to wild-type HspB1. Taking into consideration that the B1NTR protein has less quaternary structure and demonstrates more chaperone capacity for some

substrates, we propose that the availability of the NTR for Lys substrate interactions is essential to chaperone activity. Our data indicate, as exhibited by an increase in chaperone capacity of B1NTR for MDH and Lys relative to full-length HspB1, that substrate binding sites within B1NTR have chaperone activity. Furthermore, when B1NTR is decoupled from modulating quaternary dynamics, in vitro chaperone capacity increases for some, (MDH and Lys), but not all substrates. This interesting observation was not expected, but is consistent with other studies where mutations in sHsp NTRs resulted in increased chaperone activity compared to wild-type sHsps.[12]

3.3 | SEC of substrate–chaperone complexes

To determine whether B1NTR *alone* can interact with a substrate, mixtures of Lys-B1NTR or MDH-B1NTR were incubated for 1–3 h at 45°C and the distribution of species was compared to each unmixed sample (Figure 4). Samples containing 1:1 mixtures of B1NTR and MDH or Lys were allowed to incubate for an hour and were evaluated by SEC, under heat-denaturing or chemical-denaturing conditions, respectively (Figure 4A,D). The mixture containing (1:1) Lys:B1NTR resulted in SEC shifts of shorter elution volumes, relative to Lys alone. The peaks were more distinct for the mixed samples, suggesting complex formation may result in a homogenous sample (Figure 4A). SDS-PAGE evaluation of peaks from SEC indicates that B1NTR and Lys co-elute, supporting our hypothesis that a complex forms upon Lys denaturation. Similar analysis of a (1:1) MDH:B1NTR mixture resulted in shifts toward longer elution volumes and broader peaks, indicating a change in hydrodynamic radius of the protein mixture relative to each substrate or chaperone run alone (Figure 4C,D).

The co-elution of the proteins suggests that the mixtures form a complex in solution. When substrate–chaperone complexes formed, we typically observed oligomeric species that are shifted in size relative to each individual protein complex (Figure 4). As shown in Figure 4A,B, when Lys was mixed with B1NTR, a peak was observed (~20 mL, labeled “2”) that becomes sharper relative to Lys only (green), and exhibits co-elution of the protein. The appearance of Peak 2 (Figure 4A) suggests a decrease in radius relative to the unmixed sample, arising from formation of a new substrate–chaperone complex. These data indicate the Lys–B1NTR complex may be more compact relative to each protein alone in solution. These results are consistent with the chaperone activity assay where B1NTR interacts with Lys, preventing substrate aggregation (Figure 3C).

When MDH is mixed with B1NTR, a shift in the complex is observed (Figure 4C,D). Peaks 2 and 3 are shifted to larger elution volumes relative to MDH (peaks 4–6) and B1NTR alone, corresponding to a longer retention time and a complex with a smaller hydrodynamic radius. Peak fractions were evaluated by SDS-PAGE (Figure 4D), exhibiting a broad size distribution and indicated co-elution of MDH with B1NTR. Although MDH was purchased from a supplier and indicated to be pure, both the SEC and SDS-PAGE data exhibit likely contamination (Figure 4C,D). These data suggest that the interactions between B1NTR and both MDH and Lys result in changes to the hydrodynamic radius of the new species relative to each individual protein (Figure 4A,C). While the SEC shifts are subtle, the results suggest

that substrate–chaperone complexes interact with sufficient affinity to alter the observed SEC distributions of the proteins.

The SEC evaluation of the interaction between (10:1) B1NTR and CS (Figure 4E) indicates some complex formation occurs with a large excess of chaperone to substrate. Overall, the results from both the aggregation assay (Figure 3A) and SEC indicate that B1NTR exhibits chaperone capacity for CS when it is present in large excess, but no capacity is observed when less B1NTR is present (see Supporting Information Figure S5). Interestingly, B1NTR and CS co-elute over a broad range, and analysis of SEC fractions suggests several different complexes may be present. There is at least one cysteine in CS, which may form a disulfide with B1NTR upon denaturation. Similar to MDH, CS also exhibits impurities as observed by SDS-PAGE (Figure 4F). We suggest that some of the protein impurities present in CS are able to interact with B1NTR upon heating, which may contribute to the broad SEC co-elution.

3.4 | Chaperone activity of B1NTR-conjugated nanoparticles

One structural aspect of sHsps that likely contributes to their chaperone activity is their dynamic oligomerization. Many previous studies have suggested that both the oligomerization dynamics in addition to sequences of the chaperone that act as “interacting sites” contribute to the activity of sHsps.[20,61,62] Since oligomerization implies potential multivalent protein architectures, we were interested in developing a chemical system to mimic potential oligomeric states that sHsps can assume. Our rationale is that this would allow for evaluation of multivalent effects on chaperone activity of sHsps in the absence of the dynamic properties of the native system, which currently leads to indeterminate results. To determine whether the immobilization of B1NTR to AuNPs resulted in active chaperone peptides, B1NTR-AuNPs were produced by coupling purified B1NTR to 5 nm and 10 nm AuNPs coated with NHS-terminated PEG linkers. PEG linkers were inserted between the AuNP surface and the peptide to reduce potential non-specific interactions between citrate-stabilized AuNPs (unconjugated) and denaturing substrates, since prior work suggests citrate may affect sHsp chaperone activity.[63] The resulting B1NTR–AuNPs (B1NTR-NPs) were coated with ≥10 B1NTR peptides/AuNP and exhibited increased diameters, as well as altered zeta-potentials after coupling (see Supporting Information Figure S6 and Table S1). Coupling would occur between the linker and any available terminal amine on B1NTR. It is likely that multiple orientations of the peptide are presented on the NP surface.

The chaperone activity of B1NTR-NPs was evaluated using three model substrate proteins. In addition, we examined the effect of nanoparticle size on chaperone capacity of B1NTR-NPs on Lys using 5 nm and 10 nm NP conjugates. When CS was used as a substrate protein, B1NTR-NPs (10 nm) exhibited dose-dependent suppression of heat-induced CS aggregation (Figure 5A). At low concentrations of B1NTR-NP (14.9 nM), only a slight shift in aggregation was observed compared to the absence of chaperone (CS only). At higher concentrations of B1NTR-NP (29.9 nM), chaperone capacity prevented ~50% of CS aggregation. Similar to the results observed with unconjugated B1NTR, when MDH was the substrate, B1NTR-NPs demonstrated a dose-dependent suppression of aggregation. At the highest concentration of B1NTR-NP (29.9 nM), chaperone capacity prevented ~70% MDH

aggregation. In contrast to the results with CS, even very low concentrations of B1NTR-NP were able to suppress MDH aggregation (Figure 5). In contrast to the results observed for unconjugated B1NTR, the B1NTR-NPs do not alter the lag phase of CS aggregation. The observed lag phase during MDH aggregation is increased slightly, in contrast to the decrease observed when unconjugated B1NTR is used. We hypothesize that conjugation of B1NTR to the AuNPs reduces solution mobility, preventing early interactions with some of the denaturing substrates.

We evaluated the solubility of these complexes using SDS-PAGE to determine the proteins present in soluble and insoluble fractions (Figure 5C,D). Increasing concentrations of B1NTR-NP produce slight decreases in the amount of insoluble substrate protein for both CS and MDH. It is worth noting that identifying large differences in soluble versus insoluble fractions by SDS-PAGE is difficult due to potential error resulting from the heterogeneous and insoluble nature of B1NTR-NPs, which creates smearing of the visible bands. Nevertheless, we observed an increase in soluble MDH that correlated with an observed increase in chaperone activity at higher ratios of B1NTR-NPs:MDH. MDH–B1NTR and MDH–B1NTR–AuNP complexes were observed by TEM (see Supporting Information Figure S7). TEM showed a reduction in larger protein aggregates in both chaperone-containing mixtures compared to MDH only samples, consistent with our solution-phase data.

We suggest that low concentrations of nanoparticles were able to prevent aggregation of MDH in part due to their multivalent architecture, as observed for other systems.[64] It is evident that conjugating B1NTR to PEG-NPs retains chaperone activity and does not impede the binding of substrates, a necessary feature of potential sHsp mimics. Additionally, the observed differences in lag time between conjugated and non-conjugated B1NTR suggest that developing tools to probe the effects of decoupling oligomerization from sHsp-substrate binding interactions may have utility in unraveling the mechanisms of sHsp function. Our results, both with unconjugated and conjugated B1NTR, consistently suggest that the chaperone activity attributed to B1NTR is more effective when interacting with MDH compared to CS. Although both are heat-denatured substrates, this reveals that chaperone behavior is influenced by factors in addition to the type of substrate denaturation.

To exclude the possibility that the PEG linker was responsible for this effect, we tested methyl-terminated PEG-AuNPs, which have a methyl group terminating the PEG linker attached to the AuNP (in place of B1NTR, Figures 5A,B and 6B). When PEG-NP was mixed with CS, a reduction in aggregation was observed, suggesting possible formation of non-specific interactions between the PEG-NP and denaturing CS.[65] Another explanation is that the AuNP surface may not be coated perfectly by the PEG linker, allowing for interactions between the denaturing substrate and the AuNP surface. However, when PEGNP was mixed with MDH, a dramatic increase in aggregation was observed, indicating that the PEG-NPs do not contribute to any of the previously observed aggregation suppression of MDH by B1NTR-NPs. These results further indicate the presence of non-specific interactions on the surface of PEG-NPs. Control aggregation assay experiments with PEG-NPs indicate a mixture of substrate aggregates form non-specific surface interactions with NPs (Figure 6). The specific result of the interaction, either an observed increase or

decrease in aggregation, is substrate-dependent and suggests that as a substrate denatures, the unique chemical nature of the substrate drives different protein-protein interactions (Figures 5 and 6). Further examination of these non-specific effects may be worthwhile to provide additional details about the interactions between denatured proteins and the surface of conjugated nanoparticles. These studies will enable reduction of non-specific interactions, as well as development of more specific probes to study these non-enzymatic protein-protein interactions.

Additional experiments with B1NTR-NPs were performed to explore potential differences in chaperone activity due to substrate denaturation conditions. B1NTR-NPs were evaluated in the presence of Lys, which undergoes DTT-induced substrate denaturation. AuNP absorption exhibited a small peak shift from 520 nm to 518 nm after heating in the presence of substrate, indicating the occurrence of complex formation (see Supplemental Information Figure S8). In addition to the effects of B1NTR conjugation on chaperone activity, the influence of AuNP size on chaperone capacity was evaluated. B1NTR was immobilized to 5 nm and 10 nm PEG-AuNPs to compare the effects of NP size on chaperone activity. As indicated in Figure 3, unconjugated B1NTR exhibited capacity to prevent aggregation of Lys (1:1) by ~40%. Decreasing the amount of soluble B1NTR:Lys (1:2.3) did not alter the chaperone capacity of B1NTR (Figure 6A). Interestingly, when B1NTR was conjugated to 10 nm AuNPs, the results were conflicting. There was an increase in the observed lag time of initial substrate aggregation, indicating that B1NTR-NPs may facilitate, rather than reduce, aggregation. In addition, more dilute samples of B1NTR-NPs (1:500 dilution, orange curve) exhibit ~10% chaperone capacity. However, more concentrated samples (1:100 dilution, purple curve) display little to no chaperone activity, and we instead observe an increase in Lys aggregation relative to trials with no chaperone (Figure 6B). These results suggest that 10 nm B1NTR-NPs induce aggregation of Lys. Unexpectedly, when 5 nm B1NTR-NPs were evaluated under the same conditions, a concentration-dependent decrease in aggregation was observed (Figure 6C) with a corresponding shift in the lag phase. Both B1NTR-NP dilutions resulted in an overall decrease in Lys aggregation relative to unconjugated B1NTR. These data suggest that the interactions between 5 nm B1NTR-NP and Lys have changed, (relative to the experiments with 10 nm B1NTR–AuNPs) resulting in an increase in anti-aggregation capacity. For comparison, controls were performed with unconjugated 5 nm and 10 nm AuNPs (see Supporting Information Figure S9), which did not exhibit a concentration-dependent reduction in aggregation. These initial studies indicate the importance of surface interactions in contributing to chaperone activity and anti-aggregation capacity. Future studies will explore the role of protein and nanoparticle concentration, solvent, as well as other variables that are likely to affect the nature of these interactions.

4 | DISCUSSION

Although previous evidence suggests that sHsp NTRs are important for facilitating substrate interactions, our results demonstrate, for the first time, in vitro chaperone activity of the NTR of a human sHsp in the absence of the highly structured ACD and the CTR. This raises the question of how the activity of the isolated NTR reflects physiological activity of sHsps. While these results likely do not represent all of the physiological interactions of wild-type

sHsps, this study presents difficult-to-characterize evidence that sHsp NTRs directly interact with substrates and impart chaperone activity under varying conditions and concentrations.

Additionally, the present study indicates that multivalent NP probes have the ability to increase the chaperone capacity of B1NTR in vitro. Development of sHsp–NPs enables the comparison of unconjugated B1NTR to B1NTR-NPs. This provides a new approach to explore the relationship between the unfolded state of a substrate and the chaperone capacity of the sHsp, in the absence of wild-type protein dynamics. Currently, approaches to study chaperone activity do not uncouple the oligomerization dynamics from substrate binding, leaving little control over sHsp conformation. Creating chaperone-fused nanoparticles allows for more control over the system, which can be tailored to evaluate many questions about the size, shape, and multivalency of the interactions required for chaperone activity. Furthermore, our results, in combination with prior studies implicating sHsp oligomerization dynamics in chaperone activity, suggest that substrate-binding and higher-order protein structure contribute to the mechanisms of sHsp chaperone activity. The dual roles of the NTR, substrate binding and facilitating sHsp oligomerization, may contribute to regulation of the chaperone capacity of sHsps by affecting the availability of binding sites. Our studies are consistent with a model of sHsp activity where substrate binding occurs with the NTR eliciting chaperone activity. Regulation of sHsp oligomerization via the NTR may influence the available substrate interacting domains in order to modulate chaperone capacity. Increases in chaperone capacity are made possible when the NTR is involved only in substrate binding and not sHsp oligomerization. Our data also support a model for sHsp activity where the NTR is not the sole region of the sHsp involved in providing chaperone capacity, as demonstrated by the decrease in chaperone capacity for CS by B1NTR relative to wild-type HspB1.

Prior studies have implicated the NTR of sHsps in chaperone activity and substrate specificity, as well as oligomerization dynamics.[21,56,66–68] Additional work is needed to determine the specific amino acids and post-translational modifications that comprise sHsp–substrate interacting domains for different substrates. B1NTR, in the absence of the highly conserved ACD (and CTR), protected two model substrates (MDH and Lys) from aggregation at 1:1 M ratios, while no chaperone activity was observed for CS under similar conditions. Interestingly, under saturating chaperone conditions (10:1, chaperone:substrate), some aggregation of CS was prevented by B1NTR. We hypothesize that, under these conditions, the chaperone prevented CS aggregation simply by disrupting CS–CS interactions. These fascinating and unanticipated results indicate the likelihood that more than one interacting domain exists on wild-type sHsps, some of which are outside of the NTR. Additionally, these results suggest that different sHsp domains impart some level of substrate specificity. We speculate that different regions of sHsps, not just the NTR are capable of binding substrates and in fact, are likely based on our results that different substrates interact to varying degrees with the NTR. The present study also advances new insights into the role of the NTR in contributing to chaperone capacity. The observed increase in chaperone capacity of B1NTR compared to wild-type HspB1 with Lys as the substrate suggests a possible mechanism of modulation for sHsp- substrate interactions. Oligomerization or contacts made by the ACD and CTR to the NTR in the full-length protein could act to regulate substrate–sHsp interactions that are not present when the NTR

is isolated. We hypothesize that different substrates bind to different regions or sites of the sHsp and that oligomerization of sHsps contributes to substrate specificity by providing varying accessible surface contacts to promote different protein–protein interactions depending on the substrate.

Moreover, native sHsps are post-translationally modified, which has been shown to modulate their activity. Phosphorylation, in particular, is noted to contribute to sHsp activity. We suggest that using phosphorylation mimics within the truncated NTR would likely influence substrate binding due to changes in the sHsp surface properties, even in the absence of altering oligomerization dynamics of the truncated protein. Future experiments will evaluate the role of changing the physical and chemical characteristics of sites typically modified within the NTR to evaluate the role of these residues on substrate binding.

While examining the chaperone activity of B1NTR in solution, we became interested in determining whether multivalent “artificial” sHsp NTR-NP conjugates could affect the chaperone activity of B1NTR. Specifically, since oligomerization is an important and defining feature of sHsps that likely contributes to chaperone activity, we hypothesized that multivalent effects contribute to the mechanisms underlying their function. A powerful method to bioengineer potent peptide therapeutics is to fuse peptides to nanoparticles, which provides a platform for controlled molecular weight, cellular release, assembly, and multivalency.[69–72]. Previous work has demonstrated that fusing a mini-chaperone peptide to protein polymers results in chaperone-active nanoparticles that reduce apoptosis in cells.[43,45,47,73]. Additionally, since native sHsps form dynamic oligomeric structures, which at least in part contribute to activity, we hypothesized that multivalent probes using active mini-chaperones may result in in vitro chaperone activity by simulating the oligomeric scaffold to present substrate-interacting domains. In addition, these new materials would be tunable chemical probes to examine the importance of multivalent interactions, protein dynamics, and protein–protein interactions that underlie non-enzymatic chaperone activity, allowing for the investigation of sHsp function within the chaperone network. Importantly, the surface characteristics of the NPs could be tuned to possibly select for specific cellular substrates. Our initial examination of sHsp-derived NPs indicates that characteristics of the sHsp-derived peptide are retained after covalent attachment to AuNPs, as chaperone activity continued to be observed.

In summary, we demonstrate that the relatively unconserved NTR from a ubiquitous human sHsp, HspB1, is soluble and retains in vitro chaperone function in the absence of the ACD and CTR. Additionally, the B1NTR exhibits substrate specificity when comparing activity for three model substrates. Soluble B1NTR has more chaperone capacity for MDH and Lys than for CS under similar conditions. Furthermore, to investigate the role of protein quaternary structure and multivalency in chaperone activity, we designed NTR-conjugated AuNPs to simulate the function of sHsp oligomers while lacking the dynamic features of wild-type sHsps. In this first characterization of B1NTR-NPs, we determine that artificial sHsps retain in vitro chaperone activity, and also exhibit concentration-dependent decreases in substrate aggregation for MDH and Lys. The size of the AuNP contributes to the chaperone capacity of B1NTR-NPs, as demonstrated by an increase in chaperone activity with 5 nm B1NTR-NPs compared to 10 nm B1NTR-NPs. Finally, we show that B1NTR

displays substrate selectivity, as displayed by the large decrease in aggregation of MDH and Lys compared to CS. The latter result suggests that there may be more than one interacting domain on sHsps, since full-length HspB1 has greater activity toward CS. A crucial remaining question, therefore, is whether denaturing substrates interact with multiple sites on sHsps. Do different substrates interact with different combinations of sites on sHsps? Furthermore, do post-translational modifications impact substrate binding, particularly to the NTR, and, if so, how?

Multivalent B1NTR-NPs are a novel tool to facilitate studies aiming to identify and better understand chaperone-interacting-domains and have potential for multiple applications, such as creating combinatorial peptide tools, developing mini-chaperone therapeutics, and understanding the role of oligomers or multiple domains in sHsp chaperone activity. Additionally, these new chemical tools allow for important fundamental investigations into the mechanisms underlying sHsp chaperone activity, and may function as probes for non-enzymatic protein–protein interactions involved in cellular proteostasis

Supplementary Material

Refer to Web version on PubMed Central for supplementary material.

ACKNOWLEDGMENTS

The authors are deeply grateful to Dr. Jason Gestwicki (Department of Pharmaceutical Chemistry, UCSF) who kindly provided HspB1 constructs, to Blanca Carbajal Gonzalez (Microscopy Facility, MHC) for assistance in performing TEM imaging, Mahima Poreddy and Pei Liu (Mount Holyoke) for assistance with protein purification and preliminary data collection. We thank Donald Cotter and Jason Gestwicki for helpful comments during preparation of the manuscript. Funding for this work was generously provided by the Mount Holyoke College Chemistry Department and Program in Biochemistry, as well as grants to K.A.M. from the Clare Boothe Luce Foundation and from the National Institute of General Medical Sciences (R15GM120654–01).

Funding information

Henry Luce Foundation, Grant/Award Number: Clare Booth Luce Award; National Institute of General Medical Sciences, Grant/ Award Number: R15GM120654-01

Abbreviations:

HspB1	27-kDa heat shock protein
sHsps	small heat shock proteins
NTR	N-terminal region
CTR	C-terminal region
ACD	alpha-crystallin domain

REFERENCES

1. Haslbeck M, Vierling E. A first line of stress defense: small heat shock proteins and their function in protein homeostasis. J Mol Biol. 2015; 427(7):1537–1548. 10.1016/j.jmb.2015.02.002. [PubMed: 25681016]

2. Slingsby C, Clark AR. Flexible nanoassembly for sequestering non-native proteins. Structure. 2013;21(2):193–194. 10.1016/j.str.2013.01.009. [PubMed: 23394940]

3. Haslbeck M, Franzmann T, Weinfurtner D, Buchner J. Some like it hot: the structure and function of small heat-shock proteins. Nat Struct Mol Biol. 2005;12(10):842–846. 10.1038/nsmb993. [PubMed: 16205709]

4. Basha E, Lee GJ, Breci LA, et al. The identity of proteins associated with a small heat shock protein during heat stress in vivo indicates that these chaperones protect a wide range of cellular functions. J Biol Chem. 2004;279(9):7566–7575. 10.1074/jbc.M310684200. [PubMed: 14662763]

5. Perng MD, Cairns L, van den IJssel P, Prescott A, Hutcheson AM, Quinlan RA. Intermediate filament interactions can be altered by HSP27 and alphaB-crystallin. J Cell Sci. 1999;112(Pt 13): 2099–2112. [PubMed: 10362540]

6. Carra S, Alberti S, Arrigo PA, et al. The growing world of small heat shock proteins: from structure to functions. Cell Stress Chaperones. 2017;11(Pt 13):659–611. 10.1007/s12192-017-0787-8.

7. Evgrafov OV, Mersiyanova I, Irobi J, et al. Mutant small heat-shock protein 27 causes axonal Charcot-Marie-Tooth disease and distal hereditary motor neuropathy. Nat Genet. 2004;36(6):602–606. 10.1038/ng1354. [PubMed: 15122254]

8. Treweek TM, Meehan S, Ecroyd H, Carver JA. Small heat-shock proteins: important players in regulating cellular proteostasis. Cell Mol Life Sci. 2014;72(3):429–451. 10.1007/s00018-014-1754-5. [PubMed: 25352169]

9. Basha E, O'Neill H, Vierling E. Small heat shock proteins and α-crystallins: dynamic proteins with flexible functions. Trends Biochem Sci. 2011;37:1–12. 10.1016/j.tibs.2011.11.005. [PubMed: 22088262]

10. Rajagopal P, Liu Y, Shi L, Clouser AF, Klevit RE. Structure of the α-crystallin domain from the redox-sensitive chaperone, HSPB1. J Biomol NMR. 2015;63(2):223–228. 10.1007/s10858-015-9973-0. [PubMed: 26243512]

11. Basha E, Friedrich KL, Vierling E. The N-terminal arm of small heat shock proteins is important for both chaperone activity and substrate specificity. J Biol Chem. 2006;281(52):39943–39952. 10.1074/jbc.M607677200. [PubMed: 17090542]

12. Heirbaut M, Beelen S, Strelkov SV, Weeks SD. Dissecting the functional role of the N-terminal domain of the human small heat shock protein HSPB6. PLoS One. 2014;9(8):e105892 10.1371/journal.pone.0105892. [PubMed: 25157403]

13. Jehle S, Vollmar BS, Bardiaux B, et al. N-terminal domain of alphaB-crystallin provides a conformational switch for multimerization and structural heterogeneity. Proc Natl Acad Sci U S A. 2011;108(16): 6409–6414. 10.1073/pnas.1014656108. [PubMed: 21464278]

14. Delbecq SP, Rosenbaum JC, Klevit RE. A mechanism of subunit recruitment in human small heat shock protein oligomers. Biochemistry. 2015; 54(28):4276–4284. 10.1021/acs.biochem.5b00490. [PubMed: 26098708]

15. Mchaourab HS, Godar JA, Stewart PL. Structure and mechanism of protein stability sensors: chaperone activity of small heat shock proteins. Biochemistry. 2009;48(18):3828–3837. 10.1021/bi900212j. [PubMed: 19323523]

16. Haslbeck M, Ignatiou A, Saibil H, et al. A domain in the N-terminal part of Hsp26 is essential for chaperone function and oligomerization. J Mol Biol. 2004;343(2):445–455. 10.1016/j.jmb.2004.08.048. [PubMed: 15451672]

17. Kriehuber T, Rattei T, Weinmaier T, Bepperling A, Haslbeck M, Buchner J. Independent evolution of the core domain and its flanking sequences in small heat shock proteins. FASEB J. 2010;24(10): 3633–3642. 10.1096/fj.10-156992. [PubMed: 20501794]

18. Lelj-Garolla B, Mauk AG. Roles of the N- and C-terminal sequences in Hsp27 self-association and chaperone activity. Protein Sci. 2012;21(1): 122–133. 10.1002/pro.761. [PubMed: 22057845]

19. Aquilina JA, Watt SJ. The N-terminal domain of αB-crystallin is protected from proteolysis by bound substrate. Biochem Biophys Res Commun. 2007;353(4):1115–1120. 10.1016/j.bbrc.2006.12.176. [PubMed: 17207466]

20. Delbecq SP, Klevit RE. One size does not fit all: the oligomeric states of αB crystallin. FEBS Lett. 2013;587(8):1073–1080. 10.1016/j.febslet.2013.01.021. [PubMed: 23340341]

21. Fu X, Zhang H, Zhang X, et al. A dual role for the N-terminal region of Mycobacterium tuberculosis Hsp16.3 in self-oligomerization and binding denaturing substrate proteins. J Biol Chem. 2005;280(8):6337–6348. 10.1074/jbc.M406319200. [PubMed: 15545279]
22. Hochberg GKA, Ecroyd H, Liu C, et al. The structured core domain of αB-crystallin can prevent amyloid fibrillation and associated toxicity. Proc Natl Acad Sci U S A. 2014;111(16):E1562–E1570. 10.1073/pnas.1322673111. [PubMed: 24711386]
23. Jehle S, van Rossum B, Stout JR, et al. alphaB-crystallin: a hybrid solid-state/solution-state NMR investigation reveals structural aspects of the heterogeneous oligomer. J Mol Biol. 2009;385(5): 1481–1497. 10.1016/j.jmb.2008.10.097. [PubMed: 19041879]
24. Liu L, Chen J-Y, Yang B, Wang F-H, Wang Y-H, Yun C-H. Active-state structures of a small heat-shock protein revealed a molecular switch for chaperone function. Struct/Fold Des. 2015;23(11): 2066–2075. 10.1016/j.str.2015.08.015.
25. Aquilina JA, Benesch JLP, Ding LL, Yaron O, Horwitz J, Robinson CV. Phosphorylation of alphaB-crystallin alters chaperone function through loss of dimeric substructure. J Biol Chem. 2004;279(27):28675–28680. 10.1074/jbc.M403348200. [PubMed: 15117944]
26. Ecroyd H, Meehan S, Horwitz J, et al. Mimicking phosphorylation of αB-crystallin affects its chaperone activity. Biochem J. 2007;401(1): 129–141. 10.1042/BJ20060981. [PubMed: 16928191]
27. Jovcevski B, Kelly MA, Rote AP, et al. Phosphomimics destabilize Hsp27 oligomeric assemblies and enhance chaperone activity. Chem Biol. 2015; 22(2):186–195. 10.1016/j.chembiol. 2015.01.001. [PubMed: 25699602]
28. Laganowsky A, Benesch JLP, Landau M, et al. Crystal structures of truncated alphaA and alphaB crystallins reveal structural mechanisms of polydispersity important for eye lens function. Protein Sci. 2010;19(5):1031–1043. 10.1002/pro.380. [PubMed: 20440841]
29. Asomugha CO, Gupta R, Srivastava OP. Structural and functional properties of NH(2)-terminal domain, core domain, and COOH-terminal extension of αA- and αB-crystallins. Mol Vis. 2011;17:2356–2367. [PubMed: 21921988]
30. Derham BK, Harding JJ. Alpha-crystallin as a molecular chaperone. Prog Retin Eye Res. 1999;18(4):463–509. [PubMed: 10217480]
31. Kundu M, Sen PC, Das KP. Structure, stability, and chaperone function of alphaA-crystallin: role of N-terminal region. Biopolymers. 2007;86(3):177–192. 10.1002/bip.20716. [PubMed: 17345631]
32. Muranova LK, Weeks SD, Strelkov SV, Gusev NB. Characterization of mutants of human small heat shock protein HspB1 carrying replacements in the N-terminal domain and associated with hereditary motor neuron diseases. PLoS One. 2015;10(5):e0126248 10.1371/journal.pone. 0126248. [PubMed: 25965061]
33. Weeks SD, Baranova EV, Heirbaut M, et al. Molecular structure and dynamics of the dimeric human small heat shock protein HSPB6. J Struct Biol. 2014;185(3):342–354. 10.1016/j.jsb. 2013.12.009. [PubMed: 24382496]
34. Ungelenk S, Moayed F, Ho C-T, et al. Small heat shock proteins sequester misfolding proteins in near-native conformation for cellular protection and efficient refolding. Nat Commun. 2016;7:13673 10.1038/ncomms13673. [PubMed: 27901028]
35. Ahrman E, Lambert W, Aquilina JA, Robinson CV, Emanuelsson CS. Chemical cross-linking of the chloroplast localized small heat-shock protein, Hsp21, and the model substrate citrate synthase. Protein Sci. 2007;16(7):1464–1478. 10.1110/ps.072831607. [PubMed: 17567739]
36. Fu X, Shi X, Yan L, Zhang H, Chang Z. In vivo substrate diversity and preference of small heat shock protein IbpB as revealed by using a genetically incorporated photo-cross-linker. J Biol Chem. 2013;288(44):31646–31654. 10.1074/jbc.M113.501817. [PubMed: 24045939]
37. Rutsdottir G, Rasmussen IM, Hojrup P, Bernfur K, Emanuelsson C, Söderberg CAG. Chaperone-client interactions between Hsp21 and client proteins monitored in solution by small angle X-ray scattering and captured by crosslinking mass spectrometry. Protein Struct Funct Bioinformat. 2018;86(1):110–123. 10.1002/prot.25413.
38. Clark JI. Functional sequences in human alphaB crystallin. Biochim Biophys Acta. 2016;1860(1 Pt B):240–245. 10.1016/j.bbagen.2015.08.014. [PubMed: 26341790]

39. Fu X Chaperone function and mechanism of small heat-shock proteins. Acta Biochim Biophys Sin. 2014;46(5):347–356. 10.1093/abbs/gmt152. [PubMed: 24449783]
40. Specht S, Miller SBM, Mogk A, Bukau B. Hsp42 is required for sequestration of protein aggregates into deposition sites in Saccharomyces cerevisiae. J Cell Biol. 2011;195(4):617–629. 10.1083/jcb.201106037. [PubMed: 22065637]
41. Heirbaut M, Lermyte F, Martin EM, et al. Specific sequences in the N-terminal domain of human small heat-shock protein HSPB6 dictate preferential hetero-oligomerization with the orthologue HSPB1. J Biol Chem. 2017;292(24):9944–9957. 10.1074/jbc.M116.773515. [PubMed: 28487364]
42. Horwitz J Alpha-crystallin can function as a molecular chaperone. Proc Natl Acad Sci U S A. 1992;89(21):10449–10453. [PubMed: 1438232]
43. Banerjee PR, Pande A, Shekhtman A, Pande J. Molecular mechanism of the chaperone function of mini-α-crystallin, a 19-residue peptide of human α-crystallin. Biochemistry. 2015;54(2):505–515. 10.1021/bi5014479. [PubMed: 25478825]
44. Nahomi RB, DiMauro MA, Wang B, Nagaraj RH. Identification of peptides in human Hsp20 and Hsp27 that possess molecular chaperone and anti-apoptotic activities. Biochem J. 2014;465(1): 115–125. 10.1042/BJ20140837.
45. Raju M, Santhoshkumar P, Sharma KK. αA-Crystallin–Derived mini-chaperone modulates stability and function of cataract causing αAG98R-crystallin. PLoS One. 2012;7(9):e44077 10.1371/journal.pone.0044077. [PubMed: 22970163]
46. Raju M, Santhoshkumar P, Xie L, Sharma KK. Addition of αA-crystallin sequence 164–173 to a mini-chaperone DFVIFLDVKHF-SPEDLT alters the conformation but not the chaperone-like activity. Biochemistry. 2014;53(16):2615–2623. 10.1021/bi4017268. [PubMed: 24697516]
47. Sharma KK, Kumar RS, Kumar GS, Quinn PT. Synthesis and characterization of a peptide identified as a functional element in alphaA-crystallin. J Biol Chem. 2000;275(6):3767–3771. [PubMed: 10660525]
48. Slingsby C, Wistow GJ, Clark AR. Evolution of crystallins for a role in the vertebrate eye lens. Protein Sci. 2013;22(4):367–380. 10.1002/pro.2229. [PubMed: 23389822]
49. Ghosh JG, Shenoy AK, Clark JI. Interactions between important regulatory proteins and human αB crystallin †. Biochemistry. 2007;46(21): 6308–6317. 10.1021/bi700149h. [PubMed: 17487982]
50. Cloninger MJ, Bilgiçer B, Li L, Mangold SL, Phillips ST, Wolfenden ML. Multivalency. Chichester, UK: Wiley; 2012.
51. Kiessling L Synthetic multivalent ligands in the exploration of cell-surface interactions. Curr Opin Chem Biol. 2000;4(6):696–703. 10.1016/S1367-5931(00)00153-8. [PubMed: 11102876]
52. Kiessling LL, Gestwicki JE, Strong LE. Synthetic multivalent ligands as probes of signal transduction. Angew Chem Int Ed. 2006;45(15):2348–2368. 10.1002/anie.200502794.
53. Kiessling LL, Strong LE, Gestwicki JE. Principles for multivalent ligand design. Annu Rep Med Chem. 2000;35:321–330.
54. Oliveira ON, Oliveira ON Jr, Iost RM, et al. Nanomaterials for diagnosis: challenges and applications in smart devices based on molecular recognition. ACS Appl Mater Interfaces. 2014;6:14745–14766. 10.1021/am5015056. [PubMed: 24968359]
55. Miao Z, Gao Z, Chen R, Yu X, Su Z, Wei G. Surface-bioengineered gold nanoparticles for biomedical applications. Curr Med Chem. 2018;25(16):1–25. 10.2174/0929867325666180117111404.
56. Arbach H, Butler C, McMenimen KA. Chaperone activity of human small heat shock protein-GST fusion proteins. Cell Stress Chaperones. 2017;22(4):1–13. 10.1007/s12192-017-0764-2. [PubMed: 28054181]
57. Makley LN, McMenimen KA, DeVree BT, et al. Pharmacological chaperone for α-crystallin partially restores transparency in cataract models. Science. 2015;350(6261):674–677. 10.1126/science.aac9145. [PubMed: 26542570]
58. Peschek J, Braun N, Rohrberg J, et al. Regulated structural transitions unleash the chaperone activity of αB-crystallin. Proc Natl Acad Sci U S A. 2013;110(40):E3780–E3789. 10.1073/pnas.1308898110. [PubMed: 24043785]

59. Raussens V, Ruysschaert J-M, Goormaghtigh E. Protein concentration is not an absolute prerequisite for the determination of secondary structure from circular dichroism spectra: a new scaling method. Anal Biochem. 2003;319(1):114–121. [PubMed: 12842114]
60. Wiedemann C, Bellstedt P, Görlach M. CAPITO—a web server-based analysis and plotting tool for circular dichroism data. Bioinformatics. 2013;29(14):1750–1757. 10.1093/bioinformatics/btt278. [PubMed: 23681122]
61. Glover DJ, Clark DS. Oligomeric assembly is required for chaperone activity of the filamentous γ-prefoldin. FEBS J. 2015;282(15):2985–2997. 10.1111/febs.13341. [PubMed: 26096656]
62. Liu L, Chen J, Yang B, Wang Y. Oligomer-dependent and -independent chaperone activity of sHsps in different stressed conditions. FEBS Open Bio. 2015;5:155–162. 10.1016/j.fob.2015.02.006.
63. Goulet DR, Knee KM, King JA. Inhibition of unfolding and aggregation of lens protein human gamma D crystallin by sodium citrate. Exp Eye Res. 2011;93(4):371–381. 10.1016/j.exer.2011.04.011. [PubMed: 21600897]
64. Kiessling LL, Lamanna AC. Multivalency in biological systems In: Schneider MP, ed. Chemical Probes in Biology. NATO Science Series (Series II: Mathematics, Physics and Chemistry). Vol 129 Dordrecht: Springer; 2003:345–357.
65. Wu J, Wang Z, Lin W, Chen S. Investigation of the interaction between poly(ethylene glycol) and protein molecules using low field nuclear magnetic resonance. Acta Biomater. 2013;9(5):6414–6420. 10.1016/j.actbio.2013.01.006. [PubMed: 23318816]
66. Cha J-Y, Lee S-H, Seo KH, Choi YJ, Cheong MS, Son D. N-terminal arm of orchardgrass Hsp17.2 (DgHsp17.2) is essential for both in vitro chaperone activity and in vivo thermotolerance in yeast. Arch Biochem Biophys. 2016;591:18–27. 10.1016/j.abb.2015.12.011. [PubMed: 26724757]
67. Delbecq SP, Jehle S, Klevit R. Binding determinants of the small heat shock protein, αB-crystallin: recognition of the “IxI” motif. EMBO J. 2012;31(24):4587–4594. 10.1038/emboj.2012.318. [PubMed: 23188086]
68. Jaya N, Jaya N, Garcia V, Garcia V, Vierling E, Vierling E. Substrate binding site flexibility of the small heat shock protein molecular chaperones. Proc Natl Acad Sci U S A. 2009;106(37):15604–15609. 10.1073/pnas.0902177106. [PubMed: 19717454]
69. Davis ME, Chen ZG, Shin DM. Nanoparticle therapeutics: an emerging treatment modality for cancer. Nat Rev Drug Discov. 2008;7(9):771–782. 10.1038/nrd2614. [PubMed: 18758474]
70. Haag R, Kratz F. Polymer therapeutics: concepts and applications. Angew Chem Int Ed. 2006;45(8):1198–1215. 10.1002/anie.200502113.
71. Kumar A, Ma H, Zhang X, et al. Gold nanoparticles functionalized with therapeutic and targeted peptides for cancer treatment. Biomaterials. 2012;33(4):1180–1189. 10.1016/j.biomaterials.2011.10.058. [PubMed: 22056754]
72. Stuart MAC, Huck WTS, Genzer J, et al. Emerging applications of stimuli-responsive polymer materials. Nat Mater. 2010;9(2):101–113. 10.1038/nmat2614. [PubMed: 20094081]
73. Wang W, Sreekumar PG, Valluripalli V, et al. Protein polymer nanoparticles engineered as chaperones protect against apoptosis in human retinal pigment epithelial cells. J Control Release. 2014;191:4–14. [PubMed: 24780268]

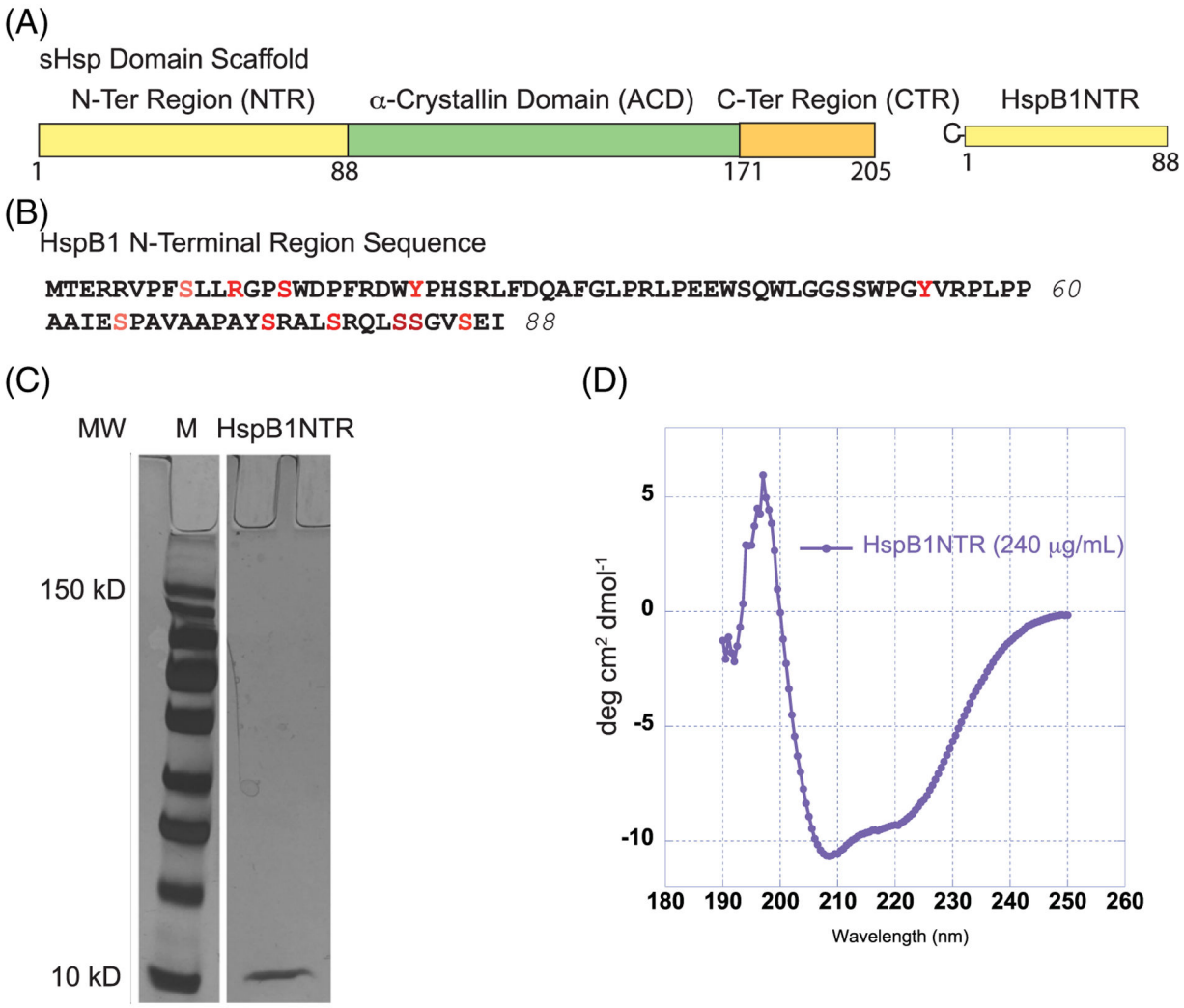

FIGURE 1.

Domain organization, sequence, and characterization of HspB1NTR. (A) sHsps are defined by three regions, the N-terminal region (NTR), a-crystallin domain (ACD), and the C-terminal region (CTR). Residues 1–88 were isolated and defined as HspB1NTR. (B) The amino acid sequence of HspB1NTR. Residues highlighted in red undergo post-translational modifications. (C) SDS-PAGE gel of purified HspB1NTR after silver stain. The protein marker highlights standards at 150 kD (highest band) and 10 kD (lowest band) while HspB1NTR is ~9.5 kD. (D) CD spectroscopy of soluble HspB1NTR (0.24 mg/mL) at 25°C in 1× PBS, pH 7.4

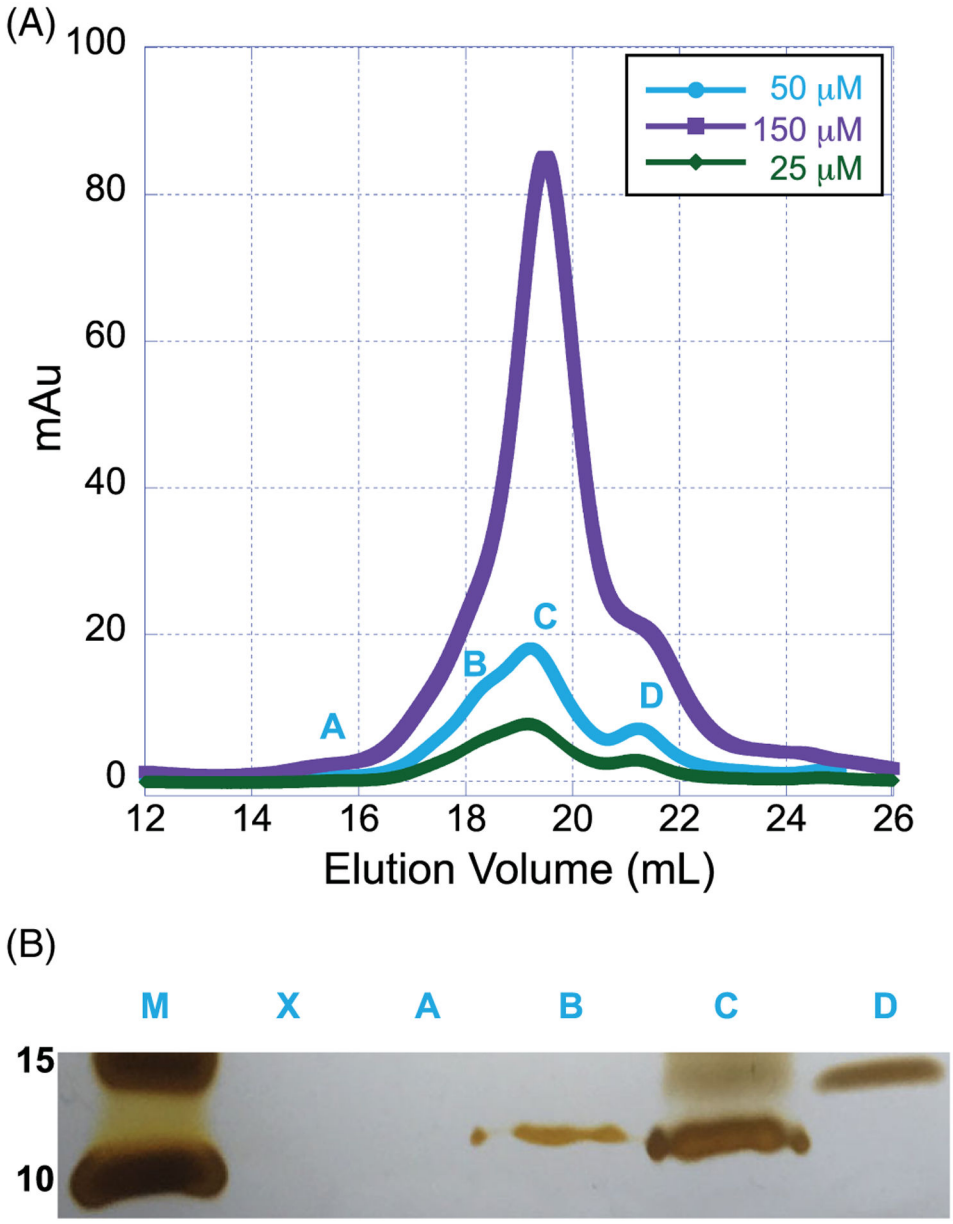

FIGURE 2.

Concentration-dependent structural changes of soluble B1NTR.(A) Concentrations of soluble, unconjugated B1NTR (25 µM [0.21 mg/mL], 50 µM [0.475 mg/mL], or 150 µM [1.47 mg/mL]) were evaluated by SEC (Superose 6 10/30 increase) at 4°C. (B) Fractions collected from SEC evaluation (A) were identified by SDS-PAGE using silver stain at 50 µM (0.476 mg/mL) of B1NTR at 25°C. Fractions contributing to each peak were collected and combined prior to removing a sample for SDS-PAGE evaluation. Protein marker is indicated (M) and relative size is listed in kDa

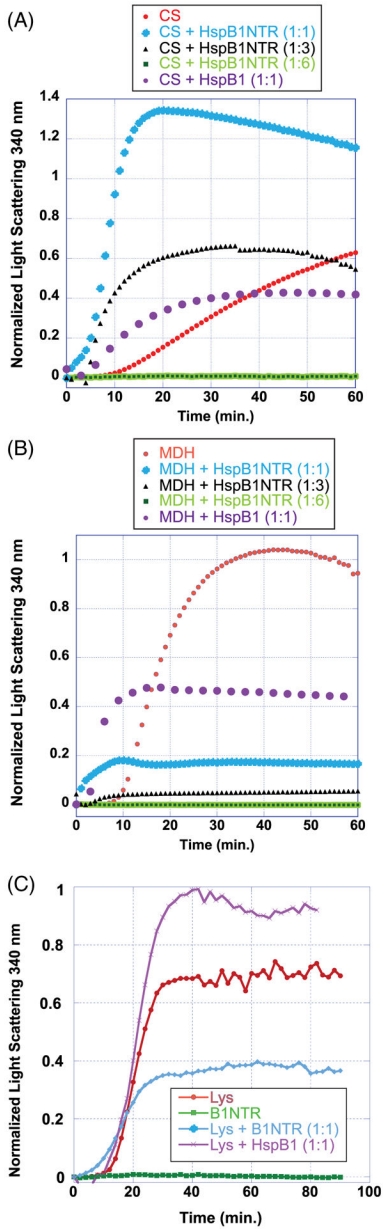

FIGURE 3.

Aggregation of denatured substrate proteins CS, MDH, and Lysozyme (Lys) in the presence of B1NTR and wild-type HspB1.(A) Heat-induced CS (2.5 μM) aggregation in the presence of 2.5, 7.5, or 15 μM B1NTR or wild-type HspB1 (2.5 μM) at 45°C. (B) Heat-induced MDH (15 μM) aggregation in the presence of 2.5, 7.5, or 15 μM B1NTR or wild-type HspB1 (2.5 μM) at 45°C. (C) DTT-induced (20 mM) aggregation of Lys (35 μM) in the presence of (35 μM) B1NTR or (35 μM) wild-type HspB1 at 37°C. Each curve is an average of ≥4 independent replicates. Data were normalized to the maximum absorbance of the averaged respective substrate-only curves in each graph

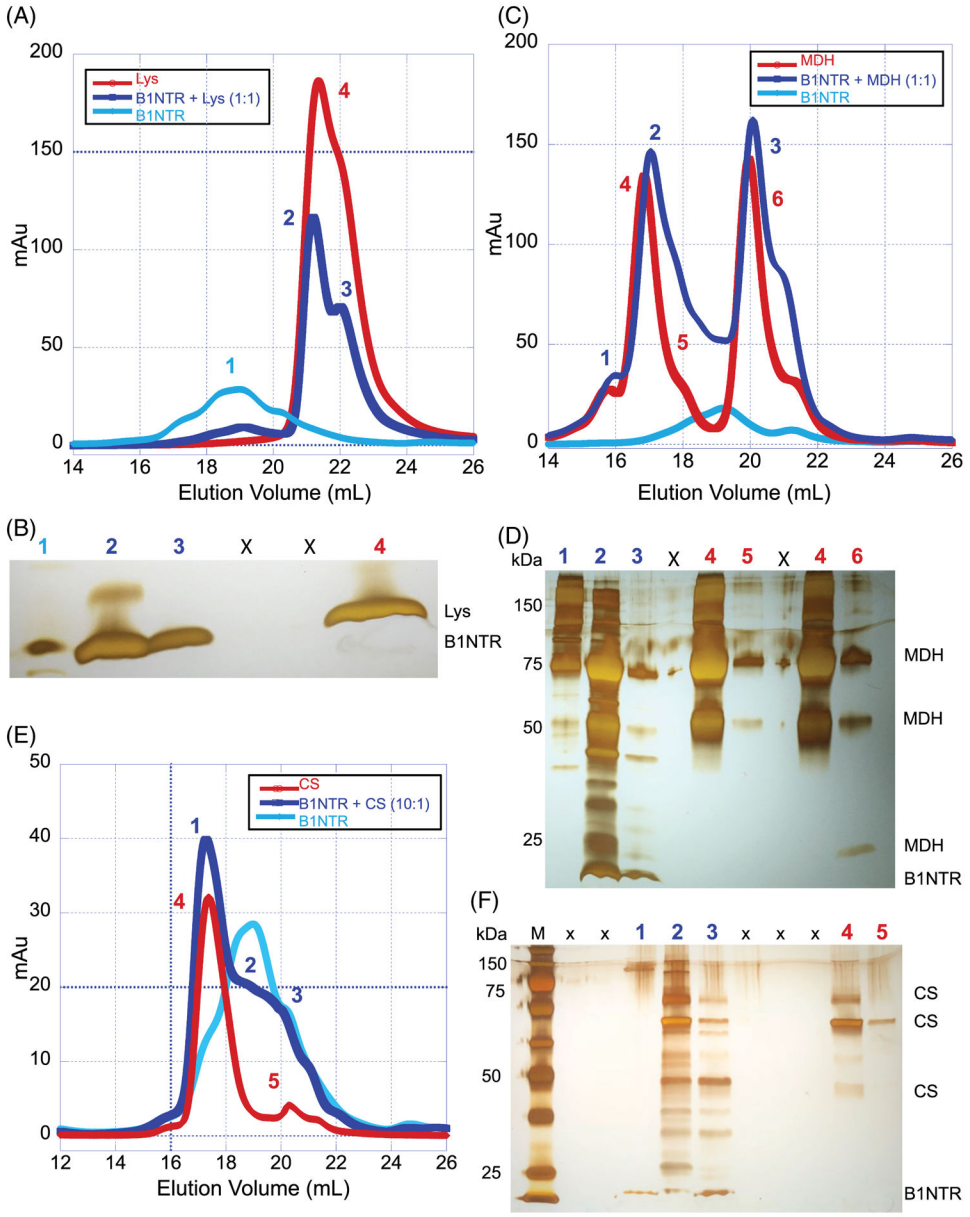

FIGURE 4.

B1NTR forms complexes with substrates during protein aggregation. (A) After incubation for 1 h at 45°C with 20 mM DTT, mixed samples of (1:1) Lys (75 μM) and B1NTR (75 μM) or each protein individually, were evaluated by SEC on a Superose 6 10/30 increase column at 0.3 mL/min. Peak fractions are indicated by numbers. (B) SDS-PAGE gel of respective sample elution fractions corresponding to observed peaks. Protein molecular mass marker is in far-left lane. Each indicated gel lane represents a sample taken from a fraction corresponding to those indicated on SEC traces, above. 1: B1NTR only, 2: B1NTR + Lys, 3: B1NTR + Lys, X: spillover lanes, 4: Lys only. (C) Mixed samples (1:1) B1NTR (50 μM) and MDH (50 μM) were evaluated by SEC after heating at 45°C for 1 h. Individual samples were obtained under similar conditions. Peak fractions are indicated by numbers above gel lanes.

(D) SDS-PAGE gel of each respective peak elution obtained from independent SEC runs. Each indicated gel lane represents a peak obtained from multiple fractions and labeled on corresponding SEC traces, above in C. (E) A 10:1 ratio of B1NTR (50 μM) and CS (5 μM) were evaluated by SEC after heating at 45°C for 1 h. Individual sample evaluations were obtained under similar conditions. Peak fractions are indicated by numbers above gel lanes. (F) SDS-PAGE gel of each respective peak elution obtained from independent SEC runs. Each indicated gel lane represents a peak obtained from multiple fractions and labeled on corresponding SEC traces, (E). M: protein molecular weight marker, X: spillover lanes, 1: B1NTR + CS, 2: B1NTR + CS, 3: B1NTR + CS, 4: CS only, 5: CS only

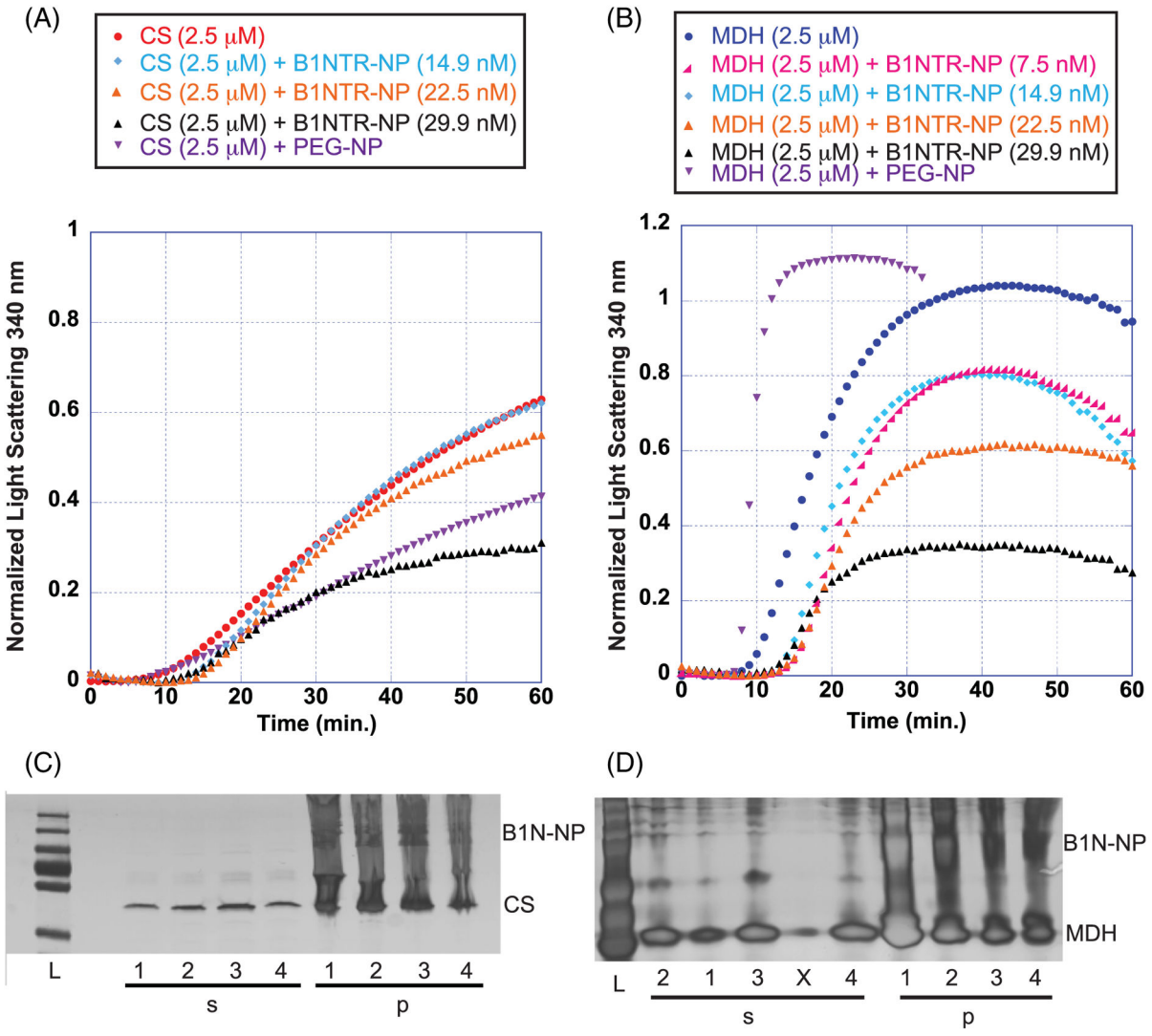

FIGURE 5.

Chaperone-like activity during heat-induced aggregation of substrates, CS and MDH. (A) Heat-induced CS (2.5 μM) aggregation in the presence of 14.9, 22.5, 29.9 nM B1NTR-NP or PEG-NP (7.48 nM) at 45°C. (B) Heat-induced MDH aggregation in the presence of 7.5, 14.9, 22.5, 29.9 nM B1NTR-NP or PEG-NP (7.48 nM) at 45°C. Each curve is an average of ≥3 replicates. (C) Mixed samples of CS (2.5 μM) and B1NTR-NP were separated into soluble (s) and insoluble (p) fractions and analyzed by SDS-PAGE after shaking for 1 h at 45°C. Samples are: (L) Molecular mass marker, (1) CS (only), (2) CS: B1NTR-NP (14.9 nM), (3) CS: B1NTR-NP (22.5 nM), (4) CS:B1NTR-NP (29.9 nM). (D) Mixed samples of MDH(2.5 μM) and B1NTR-NP were separated into soluble (s) and insoluble (p) fractions and analyzed by SDS-PAGE after shaking for 1 h at 45°C. All SDS-PAGE gels were developed using silver staining. Gel samples are: (L) Molecular mass marker, (1) MDH (only), (2) MDH: B1NTR-NP (7.5 nM),(3) MDH: B1NTR-NP (14.8), (X) spillover lane (4) MDH: B1NTR-NR (29.9 nM)

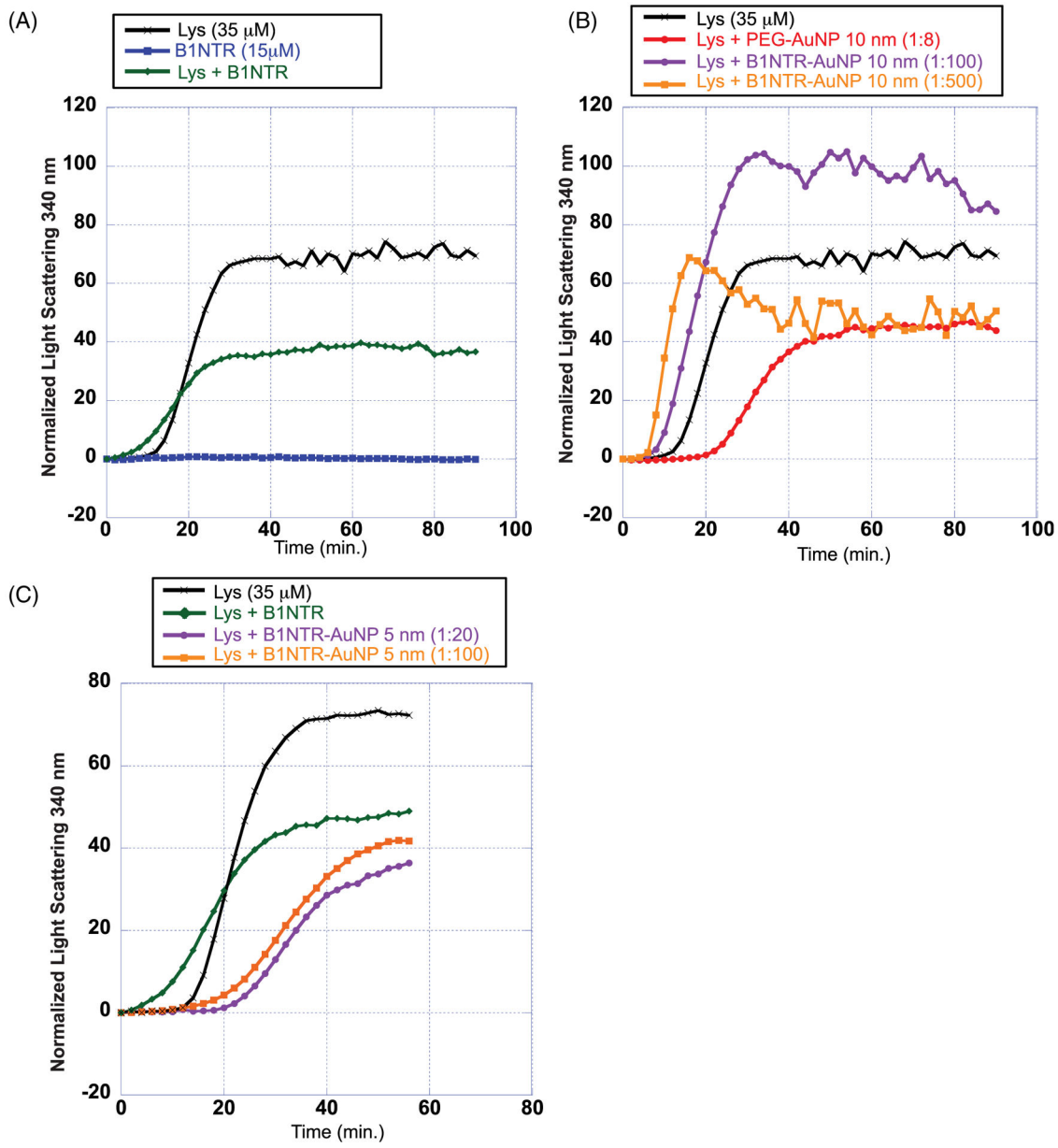

FIGURE 6.

Chemically induced aggregation of denatured lysozyme (35 μM) by DTT (20 mM) in the presence and absence of conjugated B1NTR-AuNPs. (A) Chemically induced aggregation of 35 μM Lys (black), Lys (35 μM) in presence of B1NTR (15 μM, green), and B1NTR only (15 μM, blue) with DTT (20 mM) at 37°C. (B) Aggregation of Lys in the presence of DTT (20 mM) at 37°C in the presence of conjugated B1NTR-AuNPs using 10 nm AuNPs (OD 10) at dilutions 1:100 and 1:500 (final concentration), and PEG-AuNP (1:8 dilution, 10 nm AuNP). All dilutions are calculated relative to the initial concentration of OD 10 for each 10 nm AuNP sample. All dilutions performed in 1× PBS, pH 7.4 (C) Chemically-induced aggregation of Lys (35 μM) with DTT (20 mM) at 37°C in the presence of B1NTR-AuNPs

using 5 nm AuNPs (OD 2) at final dilutions of 1:20 (purple) and 1:100 (orange) relative to starting OD 2 for each AuNP sample. Each curve is the average of ≥3 independent trials